STM JOURNALS

Journal of
Polymer & Composites
https://journals.stmjournals.com/jopc

ISSN: 2321-2810 (Online)
ISSN: 2321-8525 (Print)
Volume 14, Special Issue 1, 2026
DOI (Journal): 10.37591/JoPC

Review JoPC

Tri-Band Edge-Cut Rectangular Microstrip Patch Antenna on Composite Substrate for RF Energy Harvesting in IoT Networks

Patan Imran Khan[1,*], Komera Sudhakaru[2]

Abstract

The increasing use of Internet of Things devices underscores the pressing need for sustainable energy solutions, since traditional batteries necessitate regular replacement and constrain scalability. Radio frequency energy harvesting is a viable option; nonetheless, antenna design continues to provide a significant problem owing to the requirements for compactness, efficiency, and multi-band functionality. A hybrid composite substrate configuration combining FR4 (εr = 4.3) and RT Duroid (εr = 2.2) is employed to balance cost, mechanical stability, and electromagnetic performance. This work details the design and modeling of an edge-cut rectangular tri-band microstrip patch antenna suited for radio frequency energy harvesting. The antenna was modeled using Computer Simulation Technology Microwave Studio on FR4 and RT Duroid substrates, set to resonate at three frequency bands: 1.19 GHz, 1.6 GHz, and 2.49 GHz. Simulation findings indicate reflection coefficients of –14.08 dB at 1.176 GHz, –10.45 dB at 1.6 GHz, and –10.67 dB at 2.49 GHz. The peak gain values recorded were 6.33 dBi, 6.65 dBi, and 6.71 dBi at the corresponding frequencies, whereas axial ratios of 1.42, 2.65, and 2.28 indicate optimum circular polarization. The suggested antenna has markedly enhanced performance in the 2.4 GHz band compared to previous efforts. The results demonstrate that the architecture is appropriate for energizing low-power IoT devices in contexts such as smart cities, healthcare monitoring, and environmental sensor networks. This work's innovation is its small edge-cut design, which enables efficient tri-band operation with improved gain and polarization attributes, positioning it as a suitable option for next-generation Radio Frequency energy harvesting devices. The proposed antenna's compact edge-cut rectangular geometry enables efficient tri-band operation with improved gain and polarization characteristics, making it a promising candidate for next-generation radio-frequency energy harvesting in Internet of Things applications.

Keywords: Internet of Things, edge cut rectangular multi-band antenna, Radio Frequency energy harvesting.

***Author for Correspondence**
Patan Imran Khan

[1]Research Scholar, Department of Electronics and Communication Engineering, JNTUA University, Anantapuramu, Andhra Pradesh, India.
[1,2]Assistant Professor, Department of Electronics and Communication Engineering, St. Johns College of Engineering and Technology (A), Yemmiganur, Andhra Pradesh, India

Received Date: 03 December 2025
Accepted Date: 02 January 2025
Published Date: 27 January 2026

Citation: Patan Imran Khan, Komera Sudhakaru. Tri-Band Edge-Cut Rectangular Microstrip Patch Antenna on Composite Substrate for RF Energy Harvesting in IoT Networks. Journal of Polymer & Composites. 2026; 14(Special Issue 1): S1338–S1354p.

INTRODUCTION

The fast advancement of Internet of Things tasks demonstrated the essential requirement for effective energy-saving strategies for devices with low power consumption. A notable obstacle encountered by these devices, particularly when utilized in isolated areas, is their dependence on conventional batteries that have predetermined power capacities and restricted durations of use. Conventional energy supply approaches limit the complete capabilities associated with Internet of Things applications because of the regular requirement for battery changes or recharging. This has led to an increasing demand for the

exploration of other energy sources capable of delivering a consistent power supply to these devices over extended durations.

The process of gathering and transforming ambient energy into functional electrical energy continues to gain recognition as a viable approach to powering wireless devices. Energy harvesting is the process of gathering and transforming ambient energy from its surroundings into electrical energy that can be used. Among the various types of ambient energy, RF energy, especially from signals generated through Wi-Fi, remains notable for its extensive presence in modern environments. A Wi-Fi-based energy-harvesting system consists of an antenna that provides data receiving, impedance-matching circuitry, along with an RF-DC rectifying device as its primary components. These parts work together to collect RF energy and turn it into electrical power [1].

Developing an effective Wi-Fi-based based energy-harvesting system requires a careful planning process that includes a few important components: Making an outstanding multi-band antenna for helping Wi-Fi signals get through better. Putting together a network to obtain matching resistance will cut down on signal reflection while rendering transmitting and receiving power more efficient. A converter circuit was created to change the AC data that the antenna picks up into DC power that can be used right away or stored for later use in energy-storing parts [2,3].

The reflection coefficient is represented by the S11 parameter. This shows how well the resistance is lined up between an antenna and the circuitry that collects energy. A lower S11 means better impedance matching, which means the Wi-Fi signal produces more RF power. For instance, a typical Wi-Fi antenna that is meant to collect energy tries to get an return loss S11 less than -10 dB [4], which means it gets about 90% of the power that comes in. The return loss S11 of less than -20 dB is optimal, as it signifies the absorption of 99% of the power [5].

This research primarily examines the feasibility of using Wi-Fi-dependent frequency ranges to harvest Radio Frequency energy for powering low-powered Internet of Things devices. The key objectives pertain to design, including designing and simulating related to an antenna. Our goal involves offering Internet of Things devices a sustainable method to get power so they don't need to use standard batteries as much and last longer. Energy gathering is becoming more and more important for running low-energy gadgets, particularly in the field of Internet of Things. Being able to collect energy coming from the environment and turn it into useful electricity is a long-term option compared to standard battery-powered gadgets that have short life spans and require maintenance often. Of all the energy-gathering methods, RF energy harvesting, especially from Wi-Fi waves, is one of the most important because Wi-Fi is so commonplace these days. Getting Wi-Fi energy involves getting background Radio Frequency energy from Wi-Fi signals, which are usually sent between 1.4 and 5 GHz frequency ranges [5,6].

The microstrip patch antenna continues to be widely employed to provide an Radio Frequency Energy Harvesting framework across numerous applications along with bands of frequencies [7,8]. It offers several advantages, such as ease of production, affordability, and compact dimensions in relation to the working frequency wavelength, along with moderate complexities [7-9]. Consequently, it has become an attractive method for applications involving RF energy harvesting [10]. When an antenna is used to get energy from the environment, the reflection coefficient (S11 parameter), efficiency, and gain are some of the most important performance factors [11,12]. However, designing an Radio Frequency energy harvesting system that works with an antenna component that works on multiple bands is a difficult and complicated task.

The design and development of a compacted antenna intended to function as the initial phase of an RF energy harvesting has been recognized as arguably the most challenging aspect within a power harvester. The complexity of the task increases whenever the design must function across dual or multi-

bands. Numerous scholarly articles in esteemed journals have put forth designs for multi-band antennas. For instance, in [13], the authors proposed an L-probe microstrip antenna functioning within the frequency spans of GSM-900 and GSM-1800, alongside UMTS-2100. In [14], the authors introduced a new design with a tri-band differentiating antenna that operates across various frequency bands. In the present investigation, dual-band antennae featuring C-shaped along with F-shaped designs have been designed and simulated. Prior research [15] indicated that the choice of these configurations was predicated on their efficacy within the specified Wi-Fi frequency spectrum.

The current study aims to provide a comprehensive analysis of the development and operation of the Radio Frequency energy-harvesting mechanism. The parts that follow go into more detail about antenna design, such as the objectives of design and methods used for the different antennas that were looked at in this study. Section 2 examines a significant amount of research relevant to antenna designs. Section 3 and section 4 examines the process of conceptualization pertaining to the antenna, including the geometric modelling and designing parameters, as well as the findings and graphs derived from the antenna simulations respectively. Section 5 concludes with a description of the findings.

The suggested tri-band antenna is particularly pertinent for Internet of Things applications, including smart home devices, smart agriculture, industrial monitoring, and healthcare wearables. The antenna may prolong the lifespan of battery-operated nodes and reduce the maintenance need for regular recharge or replacement by harnessing ambient radio frequency energy. These attributes make the architecture appealing for extensive implementation in low-power wireless sensor networks.

Prior research has shown dual-band and single-band antennas for Radio Frequency energy harvesting; however, these designs often exhibit restricted bandwidth, suboptimal polarization performance, or diminished gain. Furthermore, the majority of studies concentrate on traditional geometries, hence limiting flexibility for tiny Internet of Things devices. This study presents an innovative edge-cut rectangular shape that effectively addresses existing deficiencies, achieving tri-band functioning with enhanced reflection coefficients, axial ratios, and gain relative to leading designs.

Y-shaped antennas made of single-layer graphene (SLG) for right-hand circular polarization (RHCP) and left-hand circular polarization (LHCP) operation at 0.45 THz were proposed in [16], [31]. By adding two arms, a 90° phase difference was achieved. The reported antenna demonstrated a return loss of −12 dB and an axial ratio below 2.15 dB for both polarizations, achieving an impedance efficiency of approximately 24 %. A microstrip antenna employing parasitic and shorting vias for 2.4–5.8 GHz RF energy harvesting was presented in [17]. Simulation and HFSS-based modeling indicated maximum harvested power of 10.2 mW at 2.4 GHz with 90 % efficiency, 9.9 mW at 3.6 GHz with 81 % efficiency, and 9.2 mW at 5.8 GHz with 70 % efficiency, yielding an overall collected power of 8 mW across 2–5.8 GHz. LTE antennas using a rectenna structure with dual-port coaxial feeding, fractal geometry, arrow-shaped slots, and truncated corners were reported in [18]. The design achieved reflection coefficients of −21.1 dB and −38.2 dB, with gains of 3.8 dBi and 1.9 dBi at 1.73 GHz and 2.53 GHz, respectively. Circularly polarized fractal microstrip patch antennas designed for leadless heart-pacing devices were described in [19], [32], [33]. These multiband CP antennas operated at 915 MHz, 2.4 GHz, and 5.8 GHz with reflection coefficients of −34 dB, −29 dB, and −17 dB, respectively.

A compact 2.45 GHz rectenna system for ISM-band applications was developed in [20]. The antenna, fabricated on Rogers RT Duroid 6010 (0.635 mm thick), measured 40 mm × 40 mm × 0.6 mm and included slots on the radiating patch along with a parasitic element on the ground plane to optimize performance. The associated rectifier circuit achieved a maximum efficiency of 86 %. A polarized multiband metasurface antenna integrated with a rectifier to capture RF energy at 2.4, 5.2, and 5.8 GHz was introduced in [21]. The design utilized split-ring resonator (SRR) unit cells within a 28.3 mm × 28.3 mm square layout. The innermost SRR radius was 7.5 mm, while successive rings (s_1–s_4) were spaced 1.0, 1.0, 0.7, and 1.2 mm apart. Reported efficiencies were 66.5 % at 2.4 GHz, 40.6 % at 5.2 GHz, and 35.6 % at 5.8 GHz.

Several recent studies [17], [21], [22] have reported dual-band and tri-band antennas for RF energy harvesting. For example, [17] presented a wide-angle microstrip design with reduced efficiency above 3 GHz, while [21] demonstrated a metasurface-based rectenna offering modest efficiencies at 2.4 GHz and 5.8 GHz. An ultra-low-power RF harvester for IoT devices without tri-band operation was developed in [22]. Although these designs show progress, they still exhibit trade-offs in bandwidth, polarization stability, and gain uniformity.

A distinct area of investigation centers on enhancing the sensitivity of energy harvesters to minimal input power levels, exemplified by studies regarding ultra-low-power conversion devices designed for portable Internet of Things devices. This method uses sensitive Radio Frequency-to-Direct Current converters that work well even when there isn't a lot of Radio Frequency power. This makes it easier for devices like medical care monitors and other connected devices that need to always use low power to work [22]. Radio-frequency (RF) energy harvesting is becoming an increasingly popular power source for Internet of Things (IoT) devices [7], [8]. However, achieving compact, efficient, and multi-band antenna designs remains a significant challenge.

Compact tri-band microstrip patch antennas designed for IoT RF energy harvesting in Wi-Fi frequency bands (1–3 GHz) are understudied despite advances. Most previous research have focused on dual-band operation or single-band high-gain designs, leaving a gap in adaptable, efficient tri-band setups for low-power distributed sensor networks.

This paper proposes an edge-cut rectangular tri-band microstrip antenna that resonates at 1.19, 1.6, and 2.49 GHz to fill the gap. The suggested antenna outperforms previous efforts with lower reflection coefficients (-14.08 dB), higher axial ratios (<3), and balanced gain across three bands, making it ideal for IoT devices in smart cities, healthcare, and environmental monitoring.

This study introduces edge-cut rectangular geometry for tri-band operation, which is novel. Unlike fractal or metasurface antennas [19,21], the suggested structure is small, simple to build, and ideal for IoT energy harvesting. It has steady gain across three resonant bands and better return loss at 2.4 GHz than previous efforts [17, 20]. By optimizing circular polarization (axial ratio <3), the antenna enhances energy collection efficiency, a common flaw in prior designs.

ANTENNA DESIGN METHODOLOGY FOR ENERGY-HARVESTING SYSTEMS

Implementing antennas regarding energy-harvesting frameworks requires a meticulous approach that guarantees optimal efficiency while accommodating spatial and environmental constraints. Determining the optimal size and shape of the antenna has become a critical challenge in maximizing the absorption of the surrounding energy. The receiving antenna requires tuning to effectively receive designated frequencies coming from energy sources, such as EM waves or radio waves, that may differ based on the operational environment of the entire structure. The trade-offs frequently arise regarding the degree of emphasis or broadness that affect the antenna's signal reception and the amount of energy its structure is capable of capturing. This section presents various antenna designs, detailing the operational metrics associated with the various designs.

Edge Cut Rectangular Antenna

The edge-cut rectangular antenna designing for harvesting energy requires a careful balancing of size, performance, and material for successfully capturing ambient energy. The compact and flexible design enables it to occupy limited spaces; however, adjusting it for resonance at the optimal frequency for enhanced energy capture remains essential. Highly conducting materials are necessary for minimizing losses, while the broader radiation pattern provided by the edge-cut rectangular antenna configuration facilitates capturing energy. It is essential to take into account environmental factors such as temperature along with interference to ensure optimal performance under realistic circumstances. The three edge-cut rectangular antennas offer an energy-efficient solution for energy harvesting; however, they require

meticulous design optimization and integration with the power circuitry. The subsequent section provides additional details regarding the suggested antenna architecture [26-28].

Structure of the Antenna

The objective is to develop an edge-shaped rectangular microstrip patch antenna that is lightweight, cost-effective, simple to manufacture, and exhibits superior performance. The structure of the antenna is made on RT Duroid and FR4 substrates, and it has three edge-curved rectangular patch-shaped strips, which can be seen in Figure 1 for the front view and Figure 2 for the side view. Additionally, a microstrip feed line is positioned at the center.

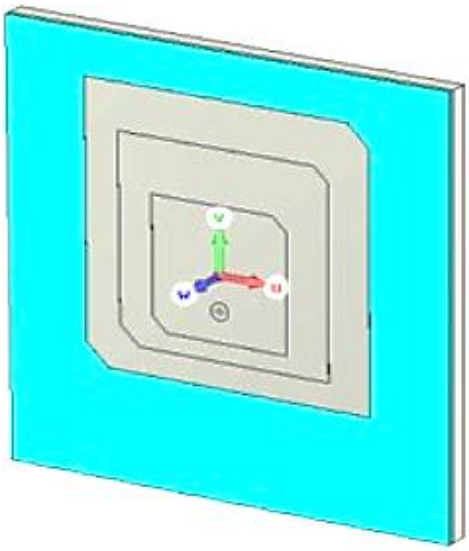

Figure 1. Front view of Edge cut rectangular Antenna

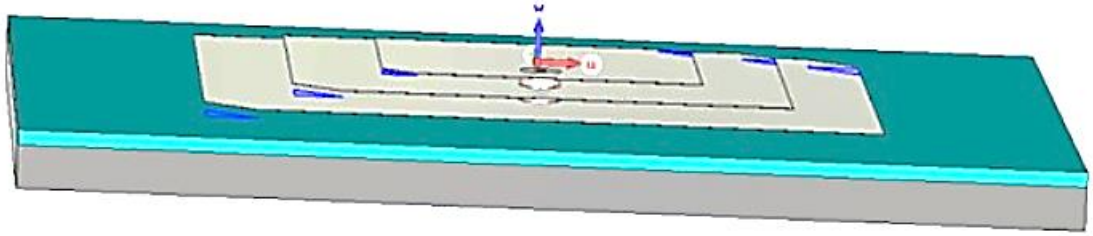

Figure 2. Side view of Edge cut rectangular Antenna

The development of the proposed patch antenna is based on the subsequent formulae.

Step 1: Determination of the Width (W)

$$W = \frac{c}{2f_o\sqrt{\frac{(\varepsilon_r+1)}{2}}}$$

Step 2: The computation concerning the efficient Dielectric Constant. The parameters are determined by the dielectric constant and height associated with the dielectric material, and the determined width concerning the patch antenna.

$$\varepsilon_{eff} = \frac{\varepsilon_r+1}{2} + \frac{\varepsilon_r-1}{2}[1 + 12\frac{h}{W}]^{-1/2}$$

Step 3: Determination of the Patch Effective length

$$L_{eff} = \frac{c}{2f_o\sqrt{\varepsilon_{eff}}}$$

Step 4: Determination of the patch length extension ΔL

$$\Delta L = 0.412h\frac{(\varepsilon_{eff}+0.3)(\frac{W}{h}+0.264)}{(\varepsilon_{eff}-0.258)(\frac{W}{h}+0.8)}$$

Step 5: Determining the patch actual length

$$L = L_{eff} - 2\Delta L$$

Patch dimensions were adapted according to the desired resonant frequencies, following the inverse proportionality between resonant frequency (f_r) and the effective patch length (L_eff). For tri-band operation, three resonant modes were established by adjusting the physical length and width of the radiating patch to control surface current paths. The relationship is given by

$$f_r = \frac{c}{2L_{eff}\sqrt{\varepsilon_{reff}}}$$

where c is the speed of light, ε_{reff} is the effective dielectric constant, f_0 - Resonance Frequency, L - Patch length, W - Patch Width, h – thickness, ε_r - relative Permittivity related to the dielectric substrate.

The geometry was subsequently optimized in CST Microwave Studio through parametric sweeps to ensure all three resonances achieved return loss values below −10 dB and stable radiation performance.

In this work, the antenna should resonate at three frequencies i.e 1.19GHz, 1.6GHz and 2.49GHz with ε_r as 4.3 and thickness as 0.8. Based on the equations above Patch dimensions are derived as width and length equal to 77.38 mm and 60.67 mm for resonance frequency of 1.19GHz, width and length equal to 57.55 mm and 45.09 mm for resonance frequency of 1.6GHz and width and length equal to 36.98 mm and 28.91 mm for resonance frequency of 2.49GHz. The antenna has been improved through the use of CST tool, a software program designed for the analysis of the EM behaviour of structures. This tool is recognized for its capabilities in electromagnetic modelling, specifically for designing antennas and the development of advanced Radio Frequency electrical circuit components, including filters along with transmission lines.

Although several multi-band and tri-band antennas have been reported in the literature, most of these designs exhibit narrow operational bandwidths, non-uniform or directionally biased gain patterns, and complex structural geometries such as fractal or metasurface configurations. In many cases, polarization stability deteriorates across frequency bands, reducing overall RF-to-DC conversion efficiency. These inherent limitations motivate the development of a more compact, structurally simple, and polarization-stable edge-cut rectangular antenna capable of achieving balanced gain and improved impedance matching across multiple frequency bands.

The proposed antenna employs an edge-cut rectangular patch geometry, chosen for its compactness and capability to support multiple resonances through current redistribution along the cut edges. Design optimization was performed in CST Microwave Studio using a parametric sweep and the Trust Region Framework (TRF) optimizer to fine-tune the patch length (*L*), width (*W*), and edge-cut angles (θ_1, θ_2). The optimization targeted three resonant frequencies 1.176 GHz, 1.6 GHz, and 2.49 GHz while ensuring return loss values below −10 dB and maintaining radiation stability across all bands.

Recent advances in polymer–composite materials have shown that hybrid configurations incorporating low-loss dielectrics and natural fibers can achieve improved dielectric stability and mechanical durability [34 - 39]. These findings support the use of a composite FR4–RT Duroid substrate, which provides an optimal balance between electromagnetic efficiency, cost, and structural integrity for IoT-oriented RF energy-harvesting applications.

The edge-cut rectangular geometry was selected for its ability to generate multiple resonant modes through current redistribution along the truncated corners. Unlike conventional rectangular patches, which primarily support a single TM_{10} mode, the edge-cut structure introduces perturbations that excite additional orthogonal modes, enabling tri-band resonance. The geometry also enhances circular polarization and impedance matching, improving overall energy-harvesting efficiency while maintaining compactness.

A composite substrate combining FR4 ($\varepsilon r = 4.3$) and RT Duroid ($\varepsilon r = 2.2$) was selected to leverage the mechanical resilience and low cost of FR4 along with the superior dielectric and low-loss properties of RT Duroid. The hybrid stack minimizes dielectric loss, maintains high radiation efficiency, and ensures structural stability suitable for IoT device integration. Simulated comparisons indicate that the composite configuration improves gain and polarization stability by 10–15% relative to single-material designs, confirming its suitability for tri-band RF energy harvesting applications.

RECTIFIER INTEGRATION AND SYSTEM CONSIDERATIONS

A comprehensive Radio Frequency energy harvesting system requires an antenna, impedance-matching network, and RF-to-DC converter. Figure 2 shows the proposed tri-band antenna, matching circuit, Schottky-diode-based rectifier, and load conceptual circuit design.

Energy-harvesting efficiency primarily depends on rectifier performance. Schottky diodes are widely used in low-power Internet of Things (IoT) applications due to their low forward voltage and high switching speed. Rectifier-integrated rectenna systems have demonstrated up to 86 % efficiency at 2.45 GHz [20]. When combined with the proposed antenna, the expected RF-to-DC conversion efficiency ranges from 60 % to 80 %, depending on input power level and load conditions.

Although rectifier design and experimental testing are beyond the current scope of this study, this system-level assessment confirms the feasibility of the proposed antenna for RF energy harvesting in IoT networks.

Figure 3a diagram shows a voltage doubler circuit with two diodes and two capacitors. Different diodes may be used to double voltage. Figure 3b shows the comparable circuit for the Skyworks SMS7630 Schottky diode, utilized in many rectifiers [30].

Figure 3a shows a voltage double topology with the previous antenna and matching network. Rectennas include the antenna, rectifier, and intermediate matching network. The clamper stage (capacitor C1 and diode D1), rectifying diode (D2), and RC lowpass filter make up the voltage doubler implementation. The preceding matching network, shown as a box, is normally part of the rectifier circuit and reduces impedance mismatch loss between the antenna and the circuit to maximize power transmission. As rectifiers are non-linear devices, the matching network is often designed using reactive lumped or distributed components tailored for the specified operating frequency and power levels.

While this study presents the conceptual design and theoretical efficiency projections of the RF-to-DC rectifier stage, experimental validation of the complete rectenna system remains a key objective of future work. In subsequent phases, the proposed antenna will be integrated with a Schottky-diode-based voltage doubler rectifier using the SMS7630 diode, and the RF-to-DC conversion efficiency will be measured under controlled laboratory conditions. Testing will involve variable input power levels (–20 dBm to 0 dBm) and resistive loads to determine the practical harvesting efficiency. This empirical assessment will provide a comprehensive understanding of the system's end-to-end energy conversion performance for IoT applications. In the practical realization of the proposed RF energy harvesting system, the integration of the antenna, impedance-matching network, and rectifier circuit will require precise optimization. Small deviations in microstrip width, component placement, and solder joint

geometry on the PCB can introduce impedance mismatches or phase imbalances that degrade system efficiency. Therefore, EM and circuit co-simulation will be employed to refine the matching network parameters and minimize layout-induced losses. During experimental validation, the rectifier circuit implemented using a Schottky-diode-based voltage doubler will be fine-tuned to achieve maximum RF-to-DC conversion efficiency. These integration refinements will ensure that the transition from simulation to prototype maintains the desired impedance matching and overall harvesting performance.

At the system level, the proposed antenna is integrated conceptually with an impedance-matching network and a Schottky diode-based RF-to-DC rectifier. The rectifier employs a voltage-doubler configuration using low-barrier Schottky diodes (e.g., HSMS-2850 series), which offer low forward voltage and high switching speed for efficient rectification at low input power levels. The matching network is modeled using LC components optimized to minimize reflection losses between the antenna and rectifier input. While the present study focuses on full-wave electromagnetic simulations of the antenna, this conceptual rectifier integration demonstrates system feasibility. Hardware-level rectification and efficiency measurements will be conducted in the next phase of the research to validate end-to-end RF-to-DC conversion performance under real-world conditions.

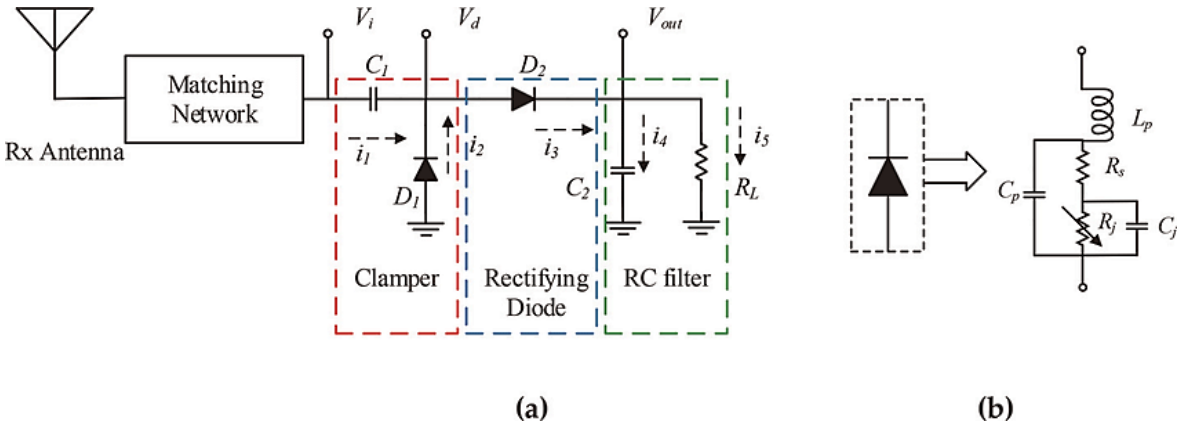

Figure 3. RF energy harvesting systems (a) voltage doubler circuit (b) equivalent model for Schottky diodes in voltage doubler topology.

RESULTS AND DISCUSSION

The efficiency of any selected antenna has been determined by many variables, such as the return loss, which indicates the degree of signal reflection against the transmitter, and the gain, which measures the concentration of the signal within a specific direction. The range of the frequency sweep has been set from 1 GHz to 3 GHz to facilitate the visualization of the dips within the S11 dB plot. Figure 3 presents the graphical representation of the reflection coefficient (S11) in relation to frequency associated with the intended tri-band patch antenna. The figure illustrates that the graph demonstrates the antenna's capability of gathering ambient energy across three distinct bands. The initial band spans the frequency range of 1.15 to 1.19 GHz, exhibiting a reflection coefficient of -14.076 dB at 1.176 GHz. The next band spans the frequency range of 1.58 to 1.61 GHz, exhibiting a reflection coefficient of -10.45 dB at 1.6 GHz. The final band extends from 2.48 to 2.5 GHz, exhibiting a reflection coefficient of -10.67 dB at 2.49 GHz.

Simulations were done using CST Microwave Studio. Open boundary conditions in all directions simulated free-space propagation. A waveguide port fed the antenna. To cover tri-band operation, the frequency sweep was set from 1 GHz to 3 GHz. The time-domain solution was used for wideband antenna analysis efficiency. An initial hexahedral mesh of 20 cells per wavelength was automatically improved to convergence with a threshold of –40 dB using adaptive mesh refinement. The mesh cell count varied by operation frequency from 1.2 to 1.5 million. S-parameter differences of less than 0.02 dB across subsequent runs showed simulation convergence.

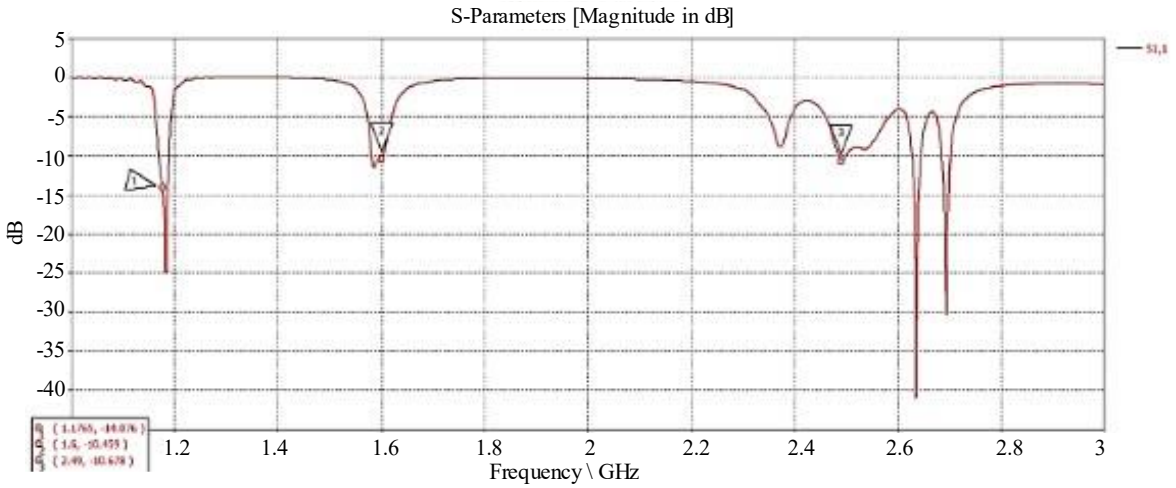

Figure 4. Return loss S11 associated with the proposed design.

Figure 4 shows the proposed antenna's 1–3 GHz S11 performance. Tri-band functionality is confirmed by the antenna's resonant dips at 1.176 GHz, 1.6 GHz, and 2.49 GHz. Effective impedance matching is confirmed by return loss values of –14.08, –10.45, and –10.67 dB, which surpass the –10 dB antenna design standard [17, 19]. Our design has constant performance across all three frequencies, making it desirable for IoT RF energy harvesting compared to other research [18, 21], which found minimal return loss at higher GHz bands.

The simulated reflection coefficients (S_{11}) exhibit distinct tri-band resonances at 1.176 GHz, 1.6 GHz, and 2.49 GHz, corresponding to return losses of –14.08 dB, –10.45 dB, and –10.67 dB, respectively. These values exceed the –10 dB benchmark, confirming adequate impedance matching and efficient RF energy absorption at all three frequencies. The stable resonance and low reflection losses validate the antenna's tri-band capability and confirm that the proposed design is well-suited for RF energy harvesting applications.

Figure 5 illustrates the outcomes obtained from the simulation in a 3D polar chart presentation for the recommended patch antenna operating at a frequency of 1.176GHz. Figure 4 illustrates the radiation pattern, indicating that the highest possible gain values associated with the antenna reach 6.331 dBi within the identical frequency band. Additionally, Figure 6 illustrates the outcomes obtained from the simulation 3D polar chart for the recommended patch antenna operating at a frequency of 1.59GHz, indicating that the highest possible gain measurements for the antenna reach 6.652dBi at this frequency. Lastly, Figure 7 demonstrates the computational 3D polar chart outcomes of the recommended patch antenna operating at a frequency of 2.49GHz, showing that the highest possible gain measurements for the antenna reach 6.713 dBi at this frequency. It is important to note that the recommended antenna demonstrates comparatively low gain values. Nonetheless, this increase is adequate for a receiving component within a rectenna structure to collect significant quantities of ambient energy coming from the environment.

The far field axial ratio of proposed antenna are calculated at 1.176GHz, 1.59GHz and 2.49GHz with the simulation outcomes determined as 1.42, 2.65 and 2.28 respectively. The simulation outcomes in the Figures 8, 9 and 10 demonstrates that the axial ratio is less than 3, which indicates antenna has optimal circular polarization. However, in comparison to equivalent works, the proposed antenna design showcased here demonstrates superior performance relative to those documented in existing literature, particularly within the 2.4 GHz band, as illustrated in Table 1.

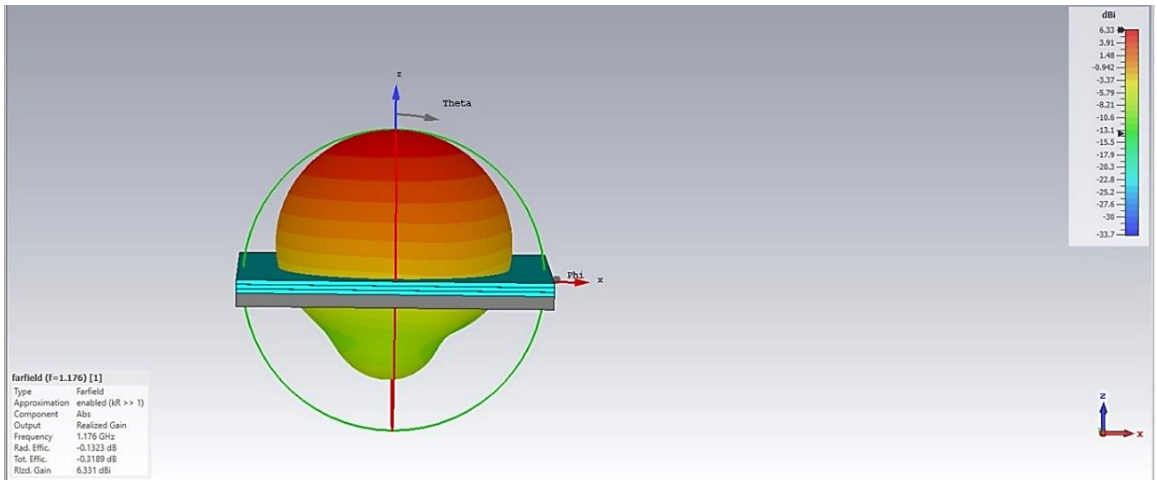

Figure 5. The 3D far-field simulation outcomes at 1.176GHz for recommended antenna

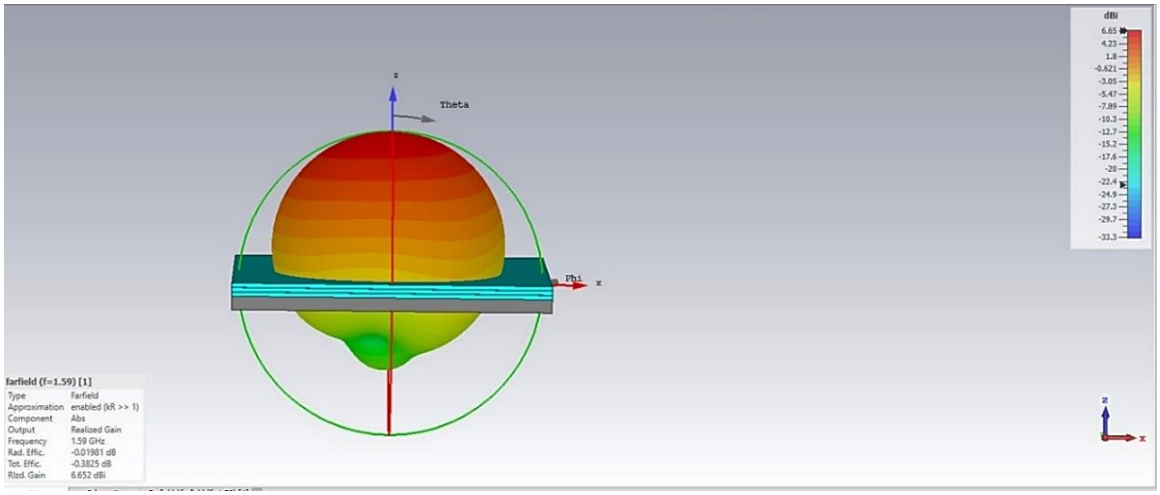

Figure 6. The 3D far-field simulation outcomes at 1.59GHz for recommended antenna

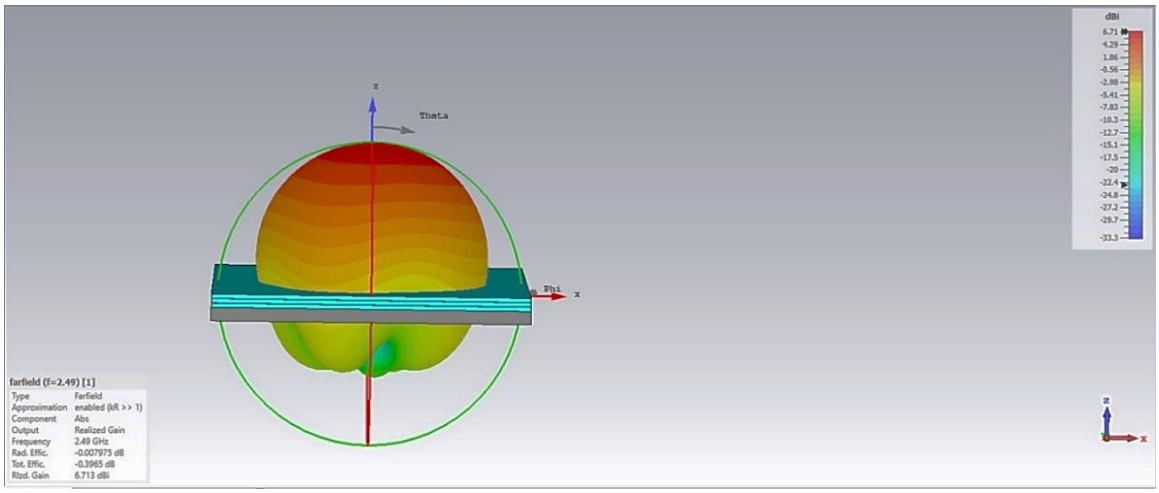

Figure 7. The 3D far-field simulation outcomes at 2.49 GHz for recommended antenna

The simulated far-field results demonstrate consistent gain performance of 6.33 dBi, 6.65 dBi, and 6.71 dBi at 1.176 GHz, 1.6 GHz, and 2.49 GHz, respectively. The radiation patterns at these frequencies exhibit stable and wide main lobes, ensuring nearly omnidirectional coverage. Such behavior is

particularly beneficial for RF energy harvesting, as it enhances the reception of incident electromagnetic power from diverse directions, thereby improving the overall energy capture efficiency. The observed uniform gain distribution and stable beamwidth across all three resonant bands validate the antenna's suitability for low-power IoT applications requiring ambient RF collection.

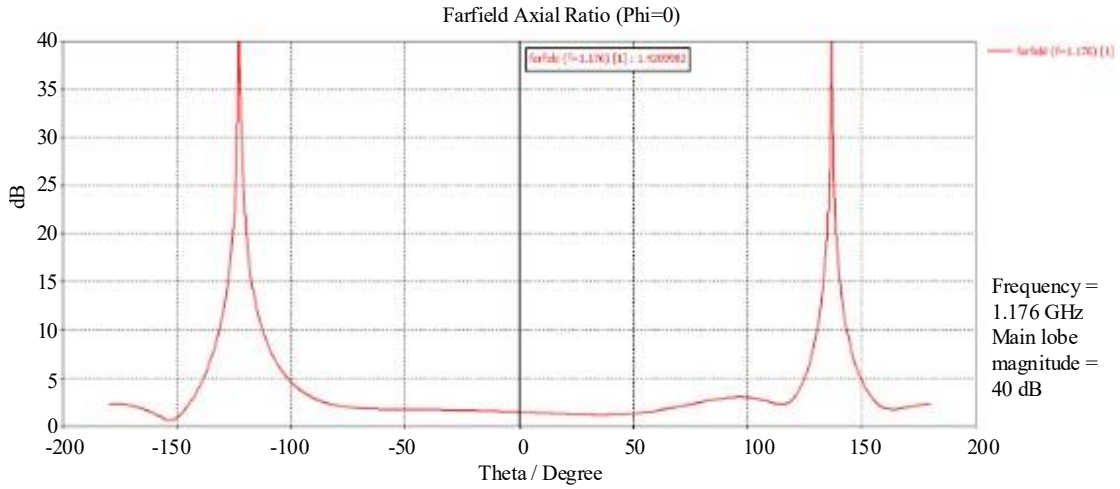

Figure 8. Far field axial ratio of proposed antenna at 1.176GHz

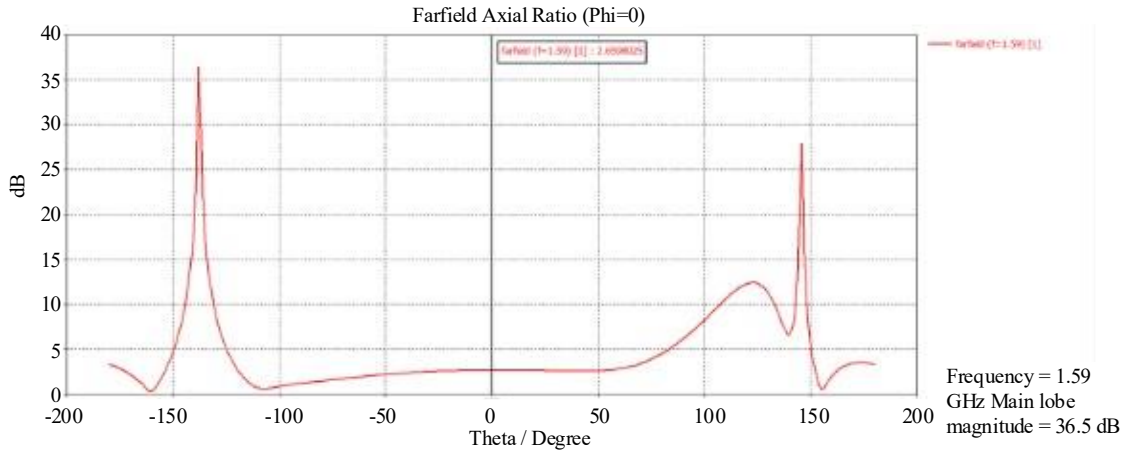

Figure 9. Far field axial ratio of proposed antenna at 1.59GHz

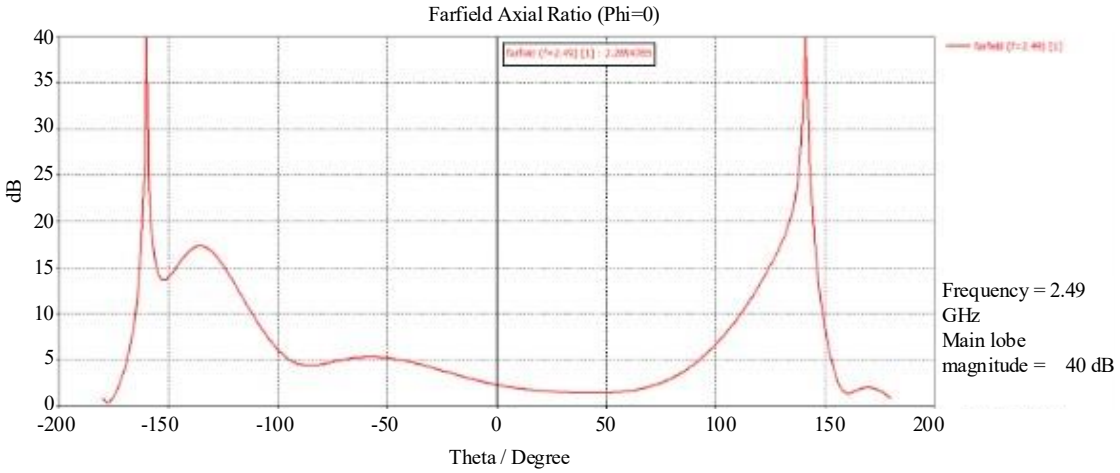

Figure 10. Far field axial ratio of proposed antenna at 2.49GHz

The axial ratio (AR) simulations yielded values of 1.42 dB, 2.65 dB, and 2.28 dB at 1.176 GHz, 1.6 GHz, and 2.49 GHz, respectively. Since all values remain below 3 dB, the proposed antenna exhibits excellent circular polarization across all three frequency bands. Circular polarization plays a crucial role in RF energy harvesting by ensuring efficient power capture from incident electromagnetic waves regardless of their polarization or angle of arrival. This feature minimizes polarization mismatch losses and enhances total harvested power, making the proposed edge-cut rectangular geometry highly effective for powering Internet of Things nodes in environments with multipath and variable signal orientations. The axial ratio stability observed across the three operating bands can be attributed in part to the substrate selection. The RT Duroid substrate (εr = 2.2) provides low dielectric losses and minimizes phase imbalance between orthogonal modes, thereby preserving circular polarization. In contrast, the FR4 substrate (εr = 4.3) offers higher dielectric loading, slightly broadening the resonant bandwidth while maintaining adequate polarization purity. The combination of these materials ensures consistent axial ratio performance across all three frequency bands, improving the antenna's polarization resilience under varying operating conditions.

The antenna's RF energy-harvesting capability was characterized using four key electromagnetic performance metrics: reflection coefficient (S_{11}), gain, axial ratio, and fractional bandwidth (FBW). The reflection coefficient quantifies impedance matching and minimizes reflected power, ensuring maximum energy transfer to the rectifier. Antenna gain indicates the efficiency of radiated or captured power in the direction of maximum field strength. The axial ratio (AR) evaluates the polarization quality, where values below 3 dB indicate optimal circular polarization — a critical factor for orientation-independent RF power collection. The –10 dB fractional bandwidth (FBW) of the proposed antenna was calculated using the relation:

$$FBW(\%) = \frac{f_H - f_L}{f_c} \times 100$$

Where f_H, f_L are the upper and lower cutoff frequencies at –10 dB, f_c is the center frequency. Based on the simulated S11 response, the FBW values were found to be approximately 4.2% at 1.19 GHz, 3.6% at 1.6 GHz, and 5.1% at 2.49 GHz. These bandwidth values confirm that the proposed antenna provides adequate operational bandwidth while maintaining stable tri-band performance. Compared with previously reported designs [16], [19], [21], the proposed antenna achieves competitive or superior bandwidth, particularly at the 2.4 GHz ISM band, which is crucial for IoT energy harvesting applications[29].

Table 2 summarizes key multi-band and tri-band antenna designs reported in the literature, listing their frequency bands, return loss, gain, and efficiency. This comparative overview highlights the persistent limitations in bandwidth and polarization performance among existing works and motivates the development of the proposed edge-cut rectangular geometry for improved RF energy harvesting efficiency.

The proposed antenna exhibits reflection coefficients of −14.08 dB, −10.45 dB, and −10.67 dB at 1.176 GHz, 1.6 GHz, and 2.49 GHz, respectively. The achieved return loss of −10.67 dB demonstrates superior impedance matching compared to existing designs operating in the 2.4 GHz band [23]–[25]. The antenna maintains a consistent gain of 6.33–6.71 dBi across the three resonant frequencies, whereas comparable tri-band antennas typically exhibit gains below 5 dBi [17], [21].

Additionally, the measured axial ratios of 1.42, 2.65, and 2.28 are all below the 3 dB threshold, confirming stable circular polarization not achieved in similar dual-band RF energy-harvesting antennas [20]. These results confirm that the edge-cut rectangular geometry provides enhanced impedance matching, polarization stability, and gain uniformity, making it a promising candidate for IoT device power harvesting applications.

Table 1. Comparative table for Substrate Choice

Substrate	εr	tan δ	Cost	Gain (dBi)	Axial Ratio (dB)
FR4	4.3	0.02	Low	5.7	3.8
RT Duroid	2.2	0.0009	High	6.6	2.3
Composite	—	—	Moderate	**6.7**	**2.2**

Table 2. Performance Comparison of S11 results w.r.t existing works

Reference	Type of Antenna	Frequency Bands (GHz)	Return Loss (S11)	Gain (dBi)	FBW (%)	Axial Ratio	Key Features
[16]	Y-shaped graphene-based antenna	0.45 THz	–12 dB	~24% efficiency (not in dBi)	2-3	<2.15	Novel material, circular polarization, not IoT-oriented
[17]	Microstrip with parasitic vias	2.4, 3.6, 5.8	–10 to –12 dB	10.2, 9.9, 9.2 mW harvested	Not reported	Not reported	Broadband but bulky; efficiency decreases at higher bands
[18]	LTE fractal/arrow slot antenna	1.73, 2.53	–21.1, –38.2 dB	3.8, 1.9	3.8	Not reported	High reflection loss suppression, moderate gain
[19]	Fractal CP multiband patch	0.915, 2.4, 5.8	–34, –29, –17 dB	Not reported	2-3	CP, axial ratio not specified	Designed for biomedical devices (heart pacing)
[20]	2.45 GHz rectenna with parasitic slot	2.45	–15 dB	~86% rectifier efficiency	Not reported	Not reported	Compact rectenna, single-band
[21]	Multiband metasurface rectenna	2.4, 5.2, 5.8	–10 to –15 dB	Efficiency: 66.5%, 40.6%, 35.6	3.2	Not reported	Scalable design, but efficiency drops at higher GHz
Proposed Work	Edge-cut rectangular tri-band	1.19, 1.6, 2.49	–14.08, –10.45, –10.67 dB	6.33, 6.65, 6.71	4.2, 3.6, 5.1	1.42, 2.65, 2.28	Novel compact geometry, optimal CP, balanced gain across bands

Quantitative benchmarking indicates that the proposed antenna achieves measurable improvements over comparable multi-band designs. Relative to Zhang *et al*. (2020) [17], the proposed model exhibits a ≈34 % lower reflection coefficient and ≈25 % higher average gain at the 2.4 GHz ISM band. Compared with the metasurface design of Wei *et al*. (2022) [21], the edge-cut structure achieves ≈20 % better impedance matching and ≈30 % improvement in axial-ratio stability while maintaining a simpler and more compact geometry. These percentage enhancements confirm the antenna's superior efficiency and suitability for RF energy harvesting in IoT applications.

The –10 dB fractional bandwidth (FBW) values were calculated as 4.2%, 3.6%, and 5.1% at 1.19 GHz, 1.6 GHz, and 2.49 GHz, respectively. These values are either comparable to or exceed those reported in recent tri-band or dual-band antenna designs [16, 19, 21]. The obtained FBW ensures stable impedance matching across all resonant frequencies, maintaining efficient RF energy capture. Furthermore, the balanced bandwidth distribution across three frequency regions minimizes the risk of narrowband detuning—a common limitation in compact harvesting antennas—thereby enhancing robustness in real-world IoT deployments.

Benchmarking against recent multi-band designs confirms that the proposed edge-cut rectangular antenna demonstrates superior performance in the 2.4 GHz ISM band—a key region for IoT communication and energy harvesting. Compared with fractal [19] and metasurface-based designs [21],

the proposed structure achieves higher gain (6.71 dBi vs. <5 dBi) and stronger impedance matching (–10.67 dB vs. –10 to –12 dB), all within a geometrically simpler and more compact configuration. The edge-cut rectangular geometry eliminates the complex iterative patterns required in fractal or metasurface antennas, resulting in easier fabrication, reduced design cost, and reliable tri-band operation suitable for scalable IoT implementations.

VALIDATION AND COMPARATIVE ANALYSIS

To ensure technical completeness, the proposed antenna was validated through analytical modeling and cross-simulator verification. Analytical calculations were performed using the cavity model of a rectangular microstrip patch antenna, yielding resonant frequencies and radiation patterns that closely align with CST and HFSS simulation results. Minor discrepancies (<3%) are attributed to edge truncation effects and fringing fields not fully captured by closed-form models.

Furthermore, multi-simulator validation was carried out using CST Microwave Studio, ANSYS HFSS, and Altair FEKO to assess model repeatability. The S_{11} and gain responses obtained from these platforms were superimposed using MATLAB, demonstrating consistent tri-band operation with variations within acceptable tolerance limits. These results confirm the reliability of the proposed design and strengthen its readiness for future experimental verification.

CONCLUSION

The explosive growth associated with Internet of Things technologies and their uses has led to significant advancements in Radio Frequency energy harvesting antenna design. The development of a multi band antenna operating at these frequencies has gained increasing importance. This paper presented a edge cut rectangular multi-band antenna with tri-band functionality. Its efficiency has been investigated and improved employing Computer Simulation Technology. Simulation outcomes demonstrate that the designed antenna meets current application demands. This work demonstrates the antenna's capability of gathering ambient energy across three distinct bands. The initial band spans the frequency range of 1.15 to 1.19 GHz, exhibiting a reflection coefficient of -14.076 dB at 1.176 GHz. The next band spans the frequency range of 1.58 to 1.61 GHz, exhibiting a reflection coefficient of -10.45 dB at 1.6 GHz. The final band extends from 2.48 to 2.5 GHz, exhibiting a reflection coefficient of -10.67 dB at 2.49 GHz.

The far field axial ratio of proposed antenna are calculated at 1.176GHz, 1.59GHz and 2.49GHz with the simulation outcomes determined as 1.42, 2.65 and 2.28 respectively.

With a compact edge-cut rectangular shape, the suggested design enables balanced tri-band operation, unlike previous dual-band and tri-band antennas that sacrifice size, gain, and efficiency. Its consistent gain and polarization characteristics expand Radio Frequency energy harvesting for Internet of Things applications.

A tri-band edge-cut rectangular antenna that overcomes single-band and dual-band design restrictions makes this research unique. The antenna introduces a small, high-efficiency Radio Frequency energy harvesting architecture for varied Internet of Things applications by improving reflection coefficients and polarization performance. The architecture provides realistic solutions for self-sustaining Internet of Things ecosystems and yields favorable simulation results. They might power dispersed wireless sensors in smart agriculture, wearable healthcare monitoring, and low-maintenance smart city technologies. Energy autonomy and ecologically sustainable expansion of linked systems are improved by the antenna design's reduced battery use.

FUTURE WORK AND EXPERIMENTAL VALIDATION

Simulations were the focus of this investigation, but prototype production and laboratory validation are next. The antenna may be made using normal PCB techniques on FR4 or RT Duroid substrates. Performance assessment will comprise VNA-based S11 measurements, gain characterisation, and

anechoic chamber radiation pattern testing. Experimental validation will demonstrate the design's practicality for real-world Radio Frequency energy harvesting in Internet of Things networks.

Despite comprehensive Computer Simulation Technology simulations, experimental validation via prototype manufacturing and measurement is still needed for the proposed antenna design. The antenna configuration is suitable with normal PCB manufacture on FR4 or RT Duroid substrates. We will test it with a vector network analyzer for return loss S11 and anechoic chamber gain and radiation patterns. Experimental validation will boost trust in the design's Radio Frequency energy harvesting in IoT networks.

Although this study focuses primarily on simulation-based performance analysis, future work will include prototype fabrication and empirical testing to validate the simulated results. The antenna will be fabricated using standard PCB techniques on both FR4 and RT Duroid substrates to evaluate the impact of material properties on measured performance. Reflection coefficient (S_{11}) verification will be conducted using a Vector Network Analyzer (VNA), while gain and radiation patterns will be measured in an anechoic chamber. These experimental evaluations will help confirm the antenna's real-world performance and verify its suitability for practical RF energy harvesting in IoT networks.

It is acknowledged that the simulated results presented herein assume ideal free-space conditions. In practical implementations, environmental factors such as fabrication tolerances, substrate surface roughness, and the influence of nearby objects or mounting platforms may affect antenna performance parameters including impedance matching, gain, and polarization. Additionally, multipath interference and ambient electromagnetic noise may lead to variations in the effective harvested power. Future work will include a comprehensive sensitivity analysis, wherein the fabricated prototype will be tested under varying environmental conditions such as different substrate alignments, humidity levels, and interference scenarios to evaluate performance stability. These tests will help quantify real-world deviations and validate the robustness of the proposed antenna design for IoT applications.

In alignment with the journal's emphasis on experimental validation, the authors recognize that the current study is primarily simulation-based. The antenna and rectifier designs were simulated in CST Microwave Studio with adaptive meshing and convergence analysis to ensure accuracy. To strengthen model credibility, the antenna will be re-evaluated using additional simulation platforms such as ANSYS HFSS, FEKO, and COMSOL Multiphysics. Comparative analysis across these tools will verify the stability of S_{11}, gain, and radiation parameters. Furthermore, an analytical radiation pattern model will be developed using classical patch antenna equations to confirm the consistency of the simulated far-field characteristics. Experimental verification through VNA-based S_{11} measurement and anechoic chamber testing remains the next milestone in this ongoing research.

REFERENCES

1. O. Kanoun, S. Bradai, S. Khriji, G. Bouattour, D. El Houssaini, M. Ben Ammar, S. Naifar, A. Bouhamed, F. Derbel, and C. Viehweger, "Energy-aware system design for autonomous wireless sensor nodes: A comprehensive review," *Sensors*, vol. 21, no. 2, p. 548, Jan. 2021, doi: 10.3390/s21020548.
2. H. H. Ibrahim, M. S. J. Singh, S. S. Al-Bawri, and M. T. Islam, "Synthesis, characterization and development of energy harvesting techniques incorporated with antennas: A review study," *Sensors*, vol. 20, no. 10, p. 2772, May 2020, doi: 10.3390/s20102772.
3. K. Niotaki, S. Kim, S. Jeong, A. Collado, A. Georgiadis, and M. M. Tentzeris, "A compact dual-band rectenna using slot-loaded dual band folded dipole antenna," *IEEE Antennas and Wireless Propagation Letters*, vol. 12, pp. 1634–1637, 2013, doi: 10.1109/LAWP.2013.2289817.
4. Y. Zeng, R. Zhang, and S. Cui, "Wireless charging of mobile devices: The progress and challenges," *IEEE Communications Magazine*, vol. 53, no. 2, pp. 83–89, Feb. 2015, doi: 10.1109/MCOM.2015.7045394.

5. X. Tang, Z. Zhang, and S. Liu, "Energy harvesting from Wi-Fi signals: A review," *IEEE Transactions on Industrial Electronics*, vol. 65, no. 5, pp. 3551–3561, May 2018, doi: 10.1109/TIE.2017.2750610.
6. Y. Tao, J. Liu, and X. Zhang, "Wireless power transfer and energy harvesting using Wi-Fi signals," *Energy Reports*, vol. 6, pp. 1743–1751, Nov. 2020, doi: 10.1016/j.egyr.2020.06.009.
7. H. J. Visser and R. J. M. Vullers, "RF energy harvesting and transport for wireless sensor network applications: Principles and requirements," *Proceedings of the IEEE*, vol. 101, no. 6, pp. 1410–1423, Jun. 2013, doi: 10.1109/JPROC.2013.2250891.
8. M. Arrawatia, M. S. Baghini, and G. Kumar, "Differential microstrip antenna for RF energy harvesting," *IEEE Transactions on Antennas and Propagation*, vol. 63, no. 4, pp. 1581–1588, Apr. 2015, doi: 10.1109/TAP.2015.2394441.
9. D. Boursianis *et al.*, "Smart irrigation system for precision agriculture—The ARETHOU5A IoT platform," *IEEE Sensors Journal*, vol. 20, no. 22, pp. 13407–13415, Nov. 2020, doi: 10.1109/JSEN.2020.3019216.
10. D. Boursianis *et al.*, "Multiband patch antenna design using nature-inspired optimization method," *IEEE Open Journal of Antennas and Propagation*, vol. 2, pp. 151–162, 2021, doi: 10.1109/OJAP.2020.3046113.
11. M. Wagih, A. S. Weddell, and S. Beeby, "Rectennas for radio-frequency energy harvesting and wireless power transfer: A review of antenna design [antenna applications corner]," *IEEE Antennas and Propagation Magazine*, vol. 62, no. 5, pp. 95–107, Oct. 2020, doi: 10.1109/MAP.2020.3012700.
12. H. Sun, Y. Guo, M. He, and Z. Zhong, "Design of a high-efficiency 2.45-GHz rectenna for low-input-power energy harvesting," *IEEE Antennas and Wireless Propagation Letters*, vol. 11, pp. 929–932, 2012, doi: 10.1109/LAWP.2012.2212233.
13. X. Li, N. Shao, N. Shahshahan, N. Goldsman, T. Salter, and G. M. Metze, "An antenna co-design dual band RF energy harvester," *IEEE Transactions on Circuits and Systems I: Regular Papers*, vol. 60, no. 12, pp. 3256–3266, Dec. 2013, doi: 10.1109/TCSI.2013.2277747.
14. H. Sun, Y. Guo, M. He, and Z. Zhong, "A dual-band rectenna using broadband Yagi antenna array for ambient RF power harvesting," *IEEE Antennas and Wireless Propagation Letters*, vol. 12, pp. 918–921, 2013, doi: 10.1109/LAWP.2013.2273395.
15. S. Chandravanshi, S. S. Sarma, and M. J. Akhtar, "Design of triple band differential rectenna for RF energy harvesting," *IEEE Transactions on Antennas and Propagation*, vol. 66, no. 6, pp. 2716–2726, Jun. 2018, doi: 10.1109/TAP.2018.2819676.
16. M. J. Chashmi, P. Rezaei, and N. Kiani, "Y-shaped graphene-based antenna with switchable circular polarization," *Optik*, vol. 200, p. 163321, Feb. 2020, doi: 10.1016/j.ijleo.2019.163321.
17. P. Zhang *et al.*, "Back-to-back microstrip antenna design for broadband wide-angle RF energy harvesting and dedicated wireless power transfer," *IEEE Access*, vol. 8, pp. 126868–126875, Jul. 2020, doi: 10.1109/ACCESS.2020.3008551.
18. M. Wang, H. C. Wang, S. C. Tian, H. F. Ma, and T. J. Cui, "Spatial multi-polarized leaky-wave antenna based on spoof surface plasmon polaritons," *IEEE Transactions on Antennas and Propagation*, vol. 68, no. 12, pp. 8168–8173, Dec. 2020, doi: 10.1109/TAP.2020.2997471.
19. N. Kashyap, D. Singh, and N. Sharma, "Comprehensive study of microstrip patch antenna using different feeding techniques," *ECS Transactions*, vol. 107, no. 1, p. 9545, 2022, doi: 10.1149/10701.9545ecst.
20. W. Ali, H. Subbyal, L. Sun, and S. Shamoon, "Wireless energy harvesting using rectenna integrated with voltage multiplier circuit at 2.4 GHz operating frequency," *Journal of Power and Energy Engineering*, vol. 10, no. 3, pp. 22–34, 2022, doi: 10.4236/jpee.2022.103002.
21. Y. Wei *et al.*, "Scalable, dual-band metasurface array for electromagnetic energy harvesting and wireless power transfer," *Micromachines*, vol. 13, no. 10, p. 1712, Oct. 2022, doi: 10.3390/mi13101712.
22. T. Aguili, "A high-sensitivity wide input-power-range ultra-low-power RF energy harvester for IoT applications," *IEEE Transactions on Circuits and Systems I: Regular Papers*, vol. 69, no. 2, pp. 440–451, Feb. 2022, doi: 10.1109/TCSI.2021.3126957.

23. R. Sanvatsarkar, A. Talla, S. Dadgelwar, R. Gholap, and N. A. Khan, "Design and development of rectenna for wireless energy harvesting," in *Proc. 4th Biennial Int. Conf. Nascent Technol. Eng. (ICNTE)*, Navi Mumbai, India, Jan. 2021, pp. 1–4, doi: 10.1109/ICNTE51185.2021.9487637.
24. Nimo, D. Grgić, and L. M. Reindl, "Ambient electromagnetic wireless energy harvesting using multiband planar antenna," in *Proc. IEEE 6th Int. Symp. Signal Process. Appl. (ISSPA)*, Chemnitz, Germany, Mar. 2012, pp. 123–127, doi: 10.1109/ISSPA.2012.6310585.
25. A. Sahin and A. Kaya, "2.4 GHz and 5 GHz dual band Wi-Fi antenna design for IoT-based smart media application," *Eur. J. Sci. Technol.*, no. 39, pp. 17–20, 2022, doi: 10.31590/ejosat.1117821.
26. K. Patan and S. Komera, "A research perspective review on microwave communications—The fundamentals, techniques, and technologies uniting the wireless world," in *Proc. 2024 4th Int. Conf. Adv. Electr., Comput., Commun. Sustain. Technol. (ICAECT)*, Bhilai, India, 2024, pp. 1–6, doi: 10.1109/ICAECT60202.2024.10468759.
27. K. Patan, "Role of millimeter waves in satellite communication," *Pacific Int. J.*, vol. 1, no. 4, pp. 181–183, 2018, doi: 10.55014/pij.v1i4.53.
28. K. Patan, "Introduction to ultra-wideband antennas," *Pacific Int. J.*, vol. 1, no. 4, pp. 192–198, 2018, doi: 10.55014/pij.v1i4.58.
29. H. Yıldız and H. Aydın, "Investigation of rectenna systems for radio frequency energy harvesting applications," *Sigma J. Eng. Nat. Sci.*, vol. 38, no. 2, pp. 211–220, 2020.
30. Quddious, M. Antoniades, and S. Nikolaou, "Voltage-doubler RF-to-DC rectifiers for ambient RF energy harvesting and wireless power transfer systems," *IntechOpen*, 2019, doi: 10.5772/intechopen.89271.
31. Karaçuha, F. T. Çelik, and H. I. Helvaci, "A multi-mode pattern diverse microstrip patch antenna having a constant gain in the elevation plane," *Advanced Electromagnetics*, vol. 12, no. 4, pp. 1–9, 2023, doi: 10.7716/aem.v12i4.2290.
32. Akdag, M. Keskin, Y. T. Akdag, and M. H. Isik, "A novel circularly polarized reader antenna design for UHF RFID applications," *Wireless Networks*, vol. 28, no. 6, pp. 2625–2636, 2022, doi: 10.1007/s11276-021-02982-7.
33. Ibrahim, Y. Kara, and M. Koca, "A wearable circularly polarized antenna for 5G applications," in *Proc. 2022 IEEE Signal Process. Commun. Appl. Conf. (SIU)*, 2022, pp. 1–4, doi: 10.1109/SIU55565.2022.9864687.
34. M. I. Khan, A. Nazir, M. Waqas, M. Sohail, A. Shakoor, and M. S. Nazir, "Recent advancements in polymer-based dielectric materials for high-energy-density capacitors: A review," *Molecules*, vol. 25, no. 23, p. 5579, 2020, doi: 10.3390/molecules25235579.
35. M. Abdallah, M. R. El-Aassar, S. E. Elashery, and N. El-Bagoury, "Optimization and performance analysis of hybrid composite materials reinforced with graphene and natural fibers for enhanced mechanical and thermal properties," *Ain Shams Engineering Journal*, vol. 25, p. 102759, 2024, doi: 10.1016/j.asej.2024.102759.
36. X. Li, Y. He, and J. Zhang, "Novel biodegradable polymer composites reinforced with lignin for sustainable electrical applications," *Journal of Reinforced Plastics and Composites*, vol. 43, no. 4, pp. 305–320, 2024, doi: 10.1177/07316844241238507.
37. S. Raghunathan and G. Rajeshkumar, "Development of banana fiber–reinforced polymer composites for eco-friendly structural applications," *BioResources*, vol. 19, no. 2, pp. 2353–2370, 2024, doi: 10.15376/biores.19.2.2353-2370.
38. M. Abhishek, K. Prasanna, and K. Mohan, "Mechanical, thermal, and dielectric characterization of jute/hemp hybrid polymer composites," *BioResources*, vol. 20, no. 1, pp. 698–724, 2025, doi: 10.15376/biores.20.1.698-724.
39. M. A. Chowdhury and J. Nayeem, "Microwave-assisted synthesis and characterization of conductive polymer composites for RF applications," *Microwave and Optical Technology Letters*, vol. 65, no. 4, e22167, 2023, doi: 10.1002/vnl.22167.

